OXFORD CENTRE FOR COLLABORATIVE APPLIED MATHEMATICS

Report Number 12/07

Axial Dispersion via Shear-enhanced Diffusion in Colloidal Suspensions

by

I. M. Griffiths, H. A. Stone

Oxford Centre for Collaborative Applied Mathematics
Mathematical Institute
24 - 29 St Giles'
Oxford
OX1 3LB
England

Axial Dispersion via Shear-enhanced Diffusion in Colloidal Suspensions

I. M. Griffiths[1,2] , H. A. Stone[1]

[1] *Department of Mechanical and Aerospace Engineering, Princeton University, Princeton, New Jersey 08544, USA*
[2] *OCCAM, Mathematical Institute, University of Oxford, Oxford, OX1 3LB*

PACS 82.70.Dd – Colloids
PACS 83.50.Ax – Shear flows (steady) rheology
PACS 83.50.Ha – Channel flow rheology

Abstract – The familiar example of Taylor dispersion of molecular solutes is extended to describe colloidal suspensions, where the fluctuations that contribute to dispersion arise from hydrodynamic interactions. The generic scheme is illustrated for a suspension of particles in a pressure-driven pipe flow, with a concentration-dependent diffusivity that captures both the shear-induced and Brownian contributions. Analytic and numerical solutions are presented that highlight the effect of the concentration dependence of this nonlinear hydrodynamic mechanism, and the results are contrasted with the classical thermally driven Taylor dispersion.

Colloidal suspensions are ubiquitous in everyday life, as they occur in many applications of soft materials [1], drug delivery systems [2], environmental science (e.g., filtration and water purification), and the flow of physiological fluids such as blood. The subject has been given renewed emphasis owing to the control offered by microfluidic devices for manipulating the flow of complex liquids [3]. In many cases, one suspension is injected into another, either in a continuous fashion or as a localized bolus. For example, the effective flow properties are needed to describe the pressure-driven flow of such suspensions [4]. In addition, the transport features of the suspension, such as the spreading of the injected pulse along the flow direction, are of interest. Traditionally, such dispersion problems are analysed assuming thermal fluctuations are the driving force for sampling the velocity distribution. For sufficiently strong shear rates in the flow, hydrodynamic effects will always dominate thermal effects, and so here we analyse the influence of hydrodynamic interactions on such dispersion problems.

It is well known that in a thin channel axial spreading of a molecular solute occurs as a consequence of a non-uniform velocity distribution in the direction transverse to the mean flow [13, 14]. Taylor dispersion refers to the common case where thermal diffusion is the source of the fluctuations that lead to sampling of the streamlines and dictates the magnitude of axial dispersion. The usual approach to axial-dispersion problems is to seek a description in terms of a one-dimensional convective-diffusion equation, with the goal being to determine the effective diffusivity. In particular, for a circular channel of radius R, or a rectangular channel of height R much less than the width, the mechanical contribution to the spreading has the order of magnitude $O\left(\overline{u}^2R^2/D_m\right)$, where $\overline{u}$ represents the average flow velocity and D_m is the molecular diffusion coefficient. For typical flow conditions, this mechanical spreading dominates the molecular diffusion and is the principal contributor to the axial spread of the solute. To accurately model the distribution of finite-sized particulates in a similar geometry requires a theory that captures the influence of hydrodynamic interactions on dispersion. In this case, determining the functional dependence of the axial dispersion coefficient on colloidal concentration is key.

For colloidal suspensions, shear-enhanced diffusion, which is a consequence of hydrodynamic interactions between particles and is dependent on the concentration of particles, dominates over thermal fluctuations (Brownian motion). Shear-enhanced diffusion is responsible for many hydrodynamic features, such as the stratification of particles in a thin film flow [16]. While there are many variants of the Taylor-dispersion problem (e.g., [15]), almost all consider only problems that assume the stochastic element driving solutes across streamlines, transverse to the flow direction, is Brownian motion. In this letter we address the effect of shear-enhanced diffusion upon the ob-

served dispersion. This description leads to a nonlinear convection-diffusion equation, with an explicit expression for the diffusivity dependence on particle concentration. We solve a simplified model analytically for low particle concentrations and numerically for higher concentrations.

In order to address the transport properties of a colloidal suspension, two main approaches have been taken: (i) models for the effective shear-enhanced diffusion coefficient [17–19], and (ii) a particle transport-based approach using suspension stresses, which accounts for axial and transverse spreading of the particles [4]. The latter model reproduces the basic features introduced originally as a shear-enhanced diffusion of colloidal objects, whereby an effective diffusivity, linear in the local shear rate, characterizes the effective flux of particles relative to the transport with the local mean velocity [17–19].

In a unidirectional flow, the characteristic shear-enhanced diffusivity for spherical particles is proportional to the local shear rate, $\dot{\gamma}$, the square of the particle radius, a, and a proportionality factor that is a function of the volume fraction of particles, which itself is related to the colloidal mass concentration, c [17, 19]. Due to the linearity and time reversibility of the Stokes flow, a purely hydrodynamic collision between two smooth non-colloidal spheres is symmetrical: the particles return to their original streamlines after the passing encounter. Thus, at least three spheres must interact to have a net displacement and, consequently, the shear-induced component of diffusivity is expected to scale as c^2 for low concentrations [18]. Non-hydrodynamic interactions such as repulsive forces, particle roughness or symmetry breaking, as in the case of non-spherical particles, leads to a diffusivity that is linear in c in the dilute limit [20, 21].

The coupling between Brownian and hydrodynamic forces due to shearing motion is non-trivial. Here we assume that the effects are additive, so that the diffusivity is represented as

$$D(c) = D_m + a^2|\dot{\gamma}|f(c), \tag{1}$$

where $f(c)$ is a dimensionless function of colloidal concentration. For spherical particles, D_m is given by the Stokes–Einstein relation, $D_m = k_BT/6\pi\mu a$, where k_B is the Boltzmann constant, T is the temperature and μ is the viscosity of the fluid in which the colloids are suspended. Eq. (1) displays the correct asymptotic behaviour in the limit of large and small colloidal sizes and shear rates. We emphasize that the steps in our analysis hold for more complex expressions for the diffusivity that capture the coupling between molecular and shear-induced diffusion.

We consider the effect of a shear-induced diffusivity on the dispersion of a colloidal suspension when placed in a steady pressure-driven pipe flow. We suppose that the pipe has radius R and length L and use an axisymmetric cylindrical coordinate system (r, z) to describe the flow, with z directed along the length of the pipe, as depicted in fig. 1.

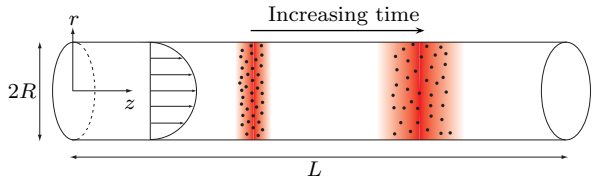

Fig. 1: Schematic diagram for pressure-driven pipe flow of a colloidal suspension.

For low colloidal concentrations, the laminar pressure-driven axial velocity profile is given by

$$u(r) = 2\overline{u}\left(1 - (r/R)^2\right), \tag{2}$$

where $\overline{u}$ is the radially averaged velocity, defined by

$$\overline{u} = \frac{2}{R^2}\int_0^R u(r)\, r\mathrm{d}r, \tag{3}$$

and the corresponding shear rate $\dot{\gamma} = \partial u/\partial r = -4\overline{u}r/R^2$. The axisymmetric colloidal mass concentration, $c(r, z, t)$, is then governed by the advection-diffusion equation,

$$\frac{\partial c}{\partial t} + u\frac{\partial c}{\partial z} = \frac{1}{r}\frac{\partial}{\partial r}\left(rD\frac{\partial c}{\partial r}\right) + \frac{\partial}{\partial z}\left(D\frac{\partial c}{\partial z}\right). \tag{4}$$

where $D(c)$ is given by (1). Following the approach of Taylor [13], we work in terms of deviations from cross-sectionally averaged quantities, defined in (3), writing $c = \overline{c}(z, t) + c'(r, z, t)$ and $u = \overline{u}(z, t) + u'(r, z, t)$. Substituting into (4) gives

$$\begin{aligned}&\frac{\partial \overline{c}}{\partial t} + \frac{\partial c'}{\partial t} + \overline{u}\frac{\partial \overline{c}}{\partial z} + u'\frac{\partial \overline{c}}{\partial z} + \overline{u}\frac{\partial c'}{\partial z} + u'\frac{\partial c'}{\partial z}\\ &= \frac{1}{r}\frac{\partial}{\partial r}\left(rD\frac{\partial c'}{\partial r}\right) + \frac{\partial}{\partial z}\left(D\frac{\partial \overline{c}}{\partial z}\right) + \frac{\partial}{\partial z}\left(D\frac{\partial c'}{\partial z}\right).\end{aligned} \tag{5}$$

Eq. 5 is averaged over the tube cross-section to provide

$$\frac{\partial \overline{c}}{\partial t} + \overline{u}\frac{\partial \overline{c}}{\partial z} + \overline{u'\frac{\partial c'}{\partial z}} = \frac{\partial}{\partial z}\left(\overline{D}\frac{\partial \overline{c}}{\partial z}\right) + \frac{\partial}{\partial z}\left(\overline{D\frac{\partial c'}{\partial z}}\right), \tag{6}$$

which may be subtracted from (5) to give

$$\begin{aligned}&\frac{\partial c'}{\partial t} + u'\frac{\partial \overline{c}}{\partial z} + \overline{u}\frac{\partial c'}{\partial z} + u'\frac{\partial c'}{\partial z} - \overline{u'\frac{\partial c'}{\partial z}} = \frac{1}{r}\frac{\partial}{\partial r}\left(rD\frac{\partial c'}{\partial r}\right)\\ &+ \frac{\partial}{\partial z}\left(\left(D - \overline{D}\right)\frac{\partial \overline{c}}{\partial z}\right) + \frac{\partial}{\partial z}\left(D\frac{\partial c'}{\partial z}\right) - \frac{\partial}{\partial z}\left(\overline{D\frac{\partial c'}{\partial z}}\right).\end{aligned} \tag{7}$$

We are interested in the long-time behaviour of cross-stream diffusion, that is, $L \gg \overline{u}R^2/D$, and we suppose that $|c'|/\overline{c} \ll 1$ so that deviations in concentration from the mean are small, under which assumptions eqs. (6) and (7) simplify to

$$\frac{\partial \overline{c}}{\partial t} + \overline{u}\frac{\partial \overline{c}}{\partial z} \approx \frac{\partial}{\partial z}\left(D(\overline{c})\frac{\partial \overline{c}}{\partial z}\right) - \overline{u'\frac{\partial c'}{\partial z}}, \tag{8}$$

and

$$\frac{1}{r}\frac{\partial}{\partial r}\left(rD(\overline{c})\frac{\partial c'}{\partial r}\right) \approx u'\frac{\partial \overline{c}}{\partial z}, \tag{9}$$

respectively. Eq. (8) corresponds to the generalization for a spatially dependent diffusivity of the usual Taylor-dispersion result. As usual, the mechanical contribution to the effective diffusion of the colloids arises from the 'fluctuation'-generated flux $\overline{u'\partial c'/\partial z}$; the influence of the shear-enhanced diffusivity enters through the functional form of this term, which is determined from (9).

Since $u'(r) = \overline{u}\left(1-2(r/R)^2\right)$, the solution of (9) satisfying $\partial c'/\partial r = 0$ on $r = 0, R$ is

$$c'(r,z,t) = \frac{\overline{u}}{12RD_mF^4}\frac{\partial \overline{c}}{\partial z}\Big\{6R^3(1-F^2)\ln\left(1+\frac{r}{R}F\right) + Fr\left[6(F^2-1)R^2+3FrR-2F^2r^2\right]\Big\} + c'(0,z,t), \tag{10}$$

where $F(\overline{c}) = Pe_s f(\overline{c})$ (with f defined in (1)) and $Pe_s = |\overline{\dot{\gamma}}|a^2/D_m$ is the particle-scale Péclet number based on the average shear rate. Thus, with u' and c' known, the mechanical contribution of the flux in (8),

$$\overline{u'\frac{\partial c'}{\partial z}} = -\frac{\overline{u}^2R^2}{D_m}\frac{\partial}{\partial z}\left(\mathcal{D}(\overline{c})\frac{\partial \overline{c}}{\partial z}\right), \tag{11}$$

where the dispersion coefficient $\mathcal{D}(\overline{c})$ is defined by

$$\mathcal{D}(\overline{c}) \equiv \frac{1}{2F^7} - \frac{1}{4F^6} - \frac{5}{6F^5} + \frac{3}{8F^4} + \frac{4}{15F^3} - \frac{1}{12F^2} + \frac{4}{105F} - \frac{\ln(1+F)}{2F^8} + \frac{\ln(1+F)}{F^6} - \frac{\ln(1+F)}{2F^4}. \tag{12}$$

We note that, since $\overline{u'} = 0$, the term $c'(0,z,t)$ in (10) does not contribute. In the limit when $F \ll 1$, the shear-enhanced component of diffusion is negligible and we recover the usual Taylor-dispersion result for the effective diffusivity, $\mathcal{D} \sim 1/48$. However, when $F \gg 1$ and the diffusion is dominated by the shear-induced contribution, we obtain the leading-order result

$$\mathcal{D}(\overline{c}) \sim \frac{4}{105F(\overline{c})} = \frac{4}{105Pe_sf(\overline{c})}. \tag{13}$$

We remark that the coefficient $4/105$ is reminiscent of the coefficient obtained for Taylor dispersion in a unidirectional parabolic channel flow between two parallel plates, though this appears only coincidentally.

Converting to a dimensionless coordinate frame that convects with the mean fluid velocity, $Ls = z - \overline{u}t$, and letting $t = D_mL^2\tau/\overline{u}^2R^2$ and $\overline{c} = MC/\pi R^2L$, where

$$M = \pi R^2\int_{-\infty}^{\infty}\overline{c}\,\mathrm{d}z \tag{14}$$

is the total number of colloids in the flow, from (8) we arrive at the non-dimensional equation for the colloidal concentration,

$$\frac{\partial C}{\partial \tau} = \frac{\partial}{\partial s}\left(\left(\frac{1}{Pe^2}\left(1+F(C)\right)+\mathcal{D}(C)\right)\frac{\partial C}{\partial s}\right), \tag{15}$$

where $Pe = \overline{u}R/D_m$ is the Péclet number based on the tube radius.

In table 1 we list typical parameters for a long microfluidic device. For all particle sizes of interest, $Pe \gg 1$, so we henceforth focus on the limit in which the dominant contribution to the diffusivity in (15) arises from the fluctuation-generated term, $\mathcal{D}$. We note that the molecular and shear-enhanced radial diffusion are respectively $O(1/Pe^2)$ and $O(Pe_s/Pe^2)$ weaker than the axial diffusion so our assumption that the concentration variations in the radial direction are small is justified.

a	R	L
$2\,\mu$m	$200\,\mu$m	50 cm

$\overline{u}$	Pe_s	Pe
$1\,\mathrm{mm\,s^{-1}}$	≈ 900	$\approx 2\times10^6$

Table 1: Typical operating parameters for $CaCO_3$ particles in water and at room temperature ($\mu = 8.9\times10^{-4}$ Pa s and $T = 298$ K) [21,22].

For dilute systems, the shear-enhanced diffusivity for perfectly smooth spherical colloids scales as C^2, while symmetry breaking or surface roughness leads to diffusivities that are linear in C [20]. We therefore begin by examining the resulting shear-enhanced dispersion in the dilute limit when $f(\overline{c}) = AC^n$ for an arbitrary n, where A is a constant. Provided C does not become too small (order $1/Pe_s$), so that F remains large, we may use the simplified expression (13) for the diffusivity. The colloidal concentration is then governed by

$$\frac{\partial C}{\partial \tau} = \frac{\partial}{\partial s}\left(\frac{1}{C^n}\frac{\partial C}{\partial s}\right), \tag{16}$$

(where we have absorbed the constant $1/(105APe_s)$ into the time variable τ), which we recognize as a version of the porous medium equation.

For an instantaneous pulse of particles injected into the flow at $s = 0$ and $\tau = 0$, the solution to (16) that conserves the total number of particles takes the form

$$C(s,\tau) = \frac{\psi(\xi_n)}{\tau^{1/(2-n)}}, \tag{17}$$

where $\xi_n = s/\tau^{1/(2-n)}$, for $0 < n < 2$. This solution form may be substituted into (16) and integrated twice to give

$$\psi(\xi_n) = \left(\frac{n}{2(2-n)}\left(\alpha_n+\xi_n^2\right)\right)^{-1/n}, \tag{18}$$

where we have used the symmetry boundary condition $\psi'(0) = 0$. Here, α_n is a constant that may be determined

by conservation of mass,

$$\int_{-\infty}^{\infty} C\,\mathrm{d}s = \int_{-\infty}^{\infty} \psi\,\mathrm{d}\xi_n = 1, \tag{19}$$

which gives

$$\alpha_n = \left(\frac{4-2n}{n}\right)^{\frac{2}{2-n}} \left(\frac{\Gamma\left(1/n\right)}{\sqrt{\pi}\Gamma\left(1/n-1/2\right)}\right)^{-\frac{2n}{2-n}}. \tag{20}$$

Thus the concentration is given by

$$C(s,\tau) = \left[\frac{n}{2(2-n)}\left(\alpha_n \tau^{n/(2-n)} + \frac{s^2}{\tau}\right)\right]^{-1/n}, \tag{21}$$

for $0 < n < 2$.

We can compare (21) with the solution for diffusion of a pulse with constant (unit) diffusivity, which is familiar in Taylor dispersion of molecular solutes,

$$C(s,\tau) = \frac{\mathrm{e}^{-s^2/4\tau}}{2\sqrt{\pi\tau}}. \tag{22}$$

In both cases, the spread advances in space as the square root of time, through the term s^2/τ. However, in (21) the spreading occurs algebraically with the height of the peak decaying as $\tau^{-1/(2-n)}$, while (22) displays an exponential spreading, with the height of the peak decaying as $\tau^{-1/2}$.

The time evolution of the solution to (16) when $n = 1$, given by (21), is compared in fig. 2(a) with the solution for diffusion of a pulse with unit diffusivity, when $n = 0$, given by (22). As a result of the stronger diffusivity in the former, the concentration distribution is smoothed out much more quickly, with the height of the peaks obeying τ^{-1} and $\tau^{-1/2}$ decay laws, respectively.

The solution (21) clearly breaks down for $n = 2$, which corresponds to the shear-enhanced diffusion of perfectly spherical particles at low concentrations lacking non-hydrodynamic interactions. In this case, the similarity solution takes the form [23, 24]

$$C(s,\tau) = \mathrm{e}^{-\omega\tau}\psi\left(\xi_2\right), \tag{23}$$

where $\xi_2 = s\mathrm{e}^{-\omega\tau}$ and ω is an, as yet, undetermined constant. Substituting (23) into (16) provides $\psi(\xi_2) = \left(\alpha_2 + \omega\xi_2^2\right)^{-1/2}$, where α_2 is a constant of integration, and so

$$C(s,\tau) = \exp\left(-\omega\tau\right)\left(\alpha_2 + \omega s^2 \mathrm{e}^{-2\omega\tau}\right)^{-1/2}. \tag{24}$$

However, the total mass associated with this solution (and (21) for $n > 2$) is unbounded. This feature arises as a result of our simplified expression for $\mathcal{D}$, which is no longer valid when C becomes small and F becomes order one. In such regions, all terms in (12) are important, and ensure that the diffusivity remains bounded as $C \to 0$. We thus conclude that the respective solutions (21) for $n > 2$ and (24) for $n = 2$ provide the behaviour in regions where the concentration is suitably larger than $O(1/Pe_s)$, but the behaviour in the tail regions of the profile, where C becomes small, is determined by using the full expression for the diffusivity, eq. (12). The constants ω and α_2 in (24) are then, in principle, determined by matching together the solutions in these two regions, and enforcing conservation of mass. Nevertheless, we observe that when $n = 2$ particles now diffuse with an exponential rather than an algebraic spread with time in regions where the colloidal concentration is not too small.

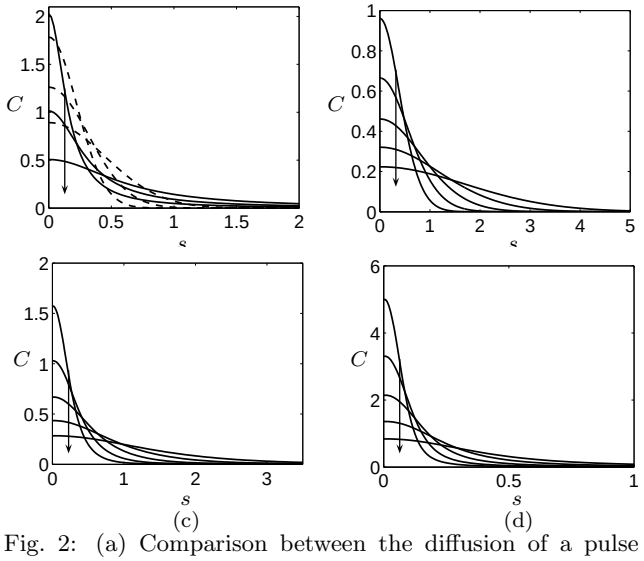

Fig. 2: (a) Comparison between the diffusion of a pulse of particles given by (21) when $n = 1$ (solid) with the solution for regular diffusion, $C = \mathrm{e}^{-s^2/4\tau}/(2\sqrt{\pi\tau})$ (dashed) at $\tau = 0.025, 0.05, 0.1$; (b) Concentration distribution, C, versus s given by (15) with (25) at $\tau = 5, 10, 20, 40, 80$ with $A = \beta = 1$ and $Pe_s = 1$, (c) $Pe_s = 10$, (d) $Pe_s = 100$. In all cases the arrows indicate the direction of increasing τ.

While the shear-enhanced component of diffusivity depends typically linearly or quadratically on concentration for low concentrations, as we increase the colloidal concentration, the diffusivity saturates [19]. Thus, we now consider a model with the more general functional form,

$$f = \frac{AC}{1+\beta C}, \qquad A,\,\beta = \text{constant}. \tag{25}$$

The solution of (15) with (25) may be determined numerically. For computational simplicity, we approximate the initial pulse of colloidal particles as a Gaussian distribution of the form $C(\zeta, 0) = \mathrm{e}^{-s^2/\tau_0}/\sqrt{\pi\tau_0}$, where $\tau_0 \ll 1$. In fig. 2(b)–(d) we illustrate the time evolution of a pulse of colloidal particles with $\tau_0 = 10^{-4}$, when $A = \beta = 1$ and $Pe_s = 1, 10, 100$. While these results illustrate the behaviour, this model may be improved by including the dependence of viscosity upon concentration, which will enter through a modification in $f(c)$.

In summary, the results reported here demonstrate that the hydrodynamic interactions which drive fluctuations in the concentration of a colloidal suspension yield a non-

linear transport process. The behaviour depends on the explicit features characterizing the functional relation between shear-induced diffusivity and colloidal concentration. The approach presented may be used to refine the standard dispersion methods used to determine the diffusion coefficients for colloids and nanoparticles (see, for example, [25, 26]). Furthermore, the ideas here may be useful for other problems involving transport properties of colloidal suspensions, such as sedimentation and membrane filtration [27, 28], as well as cases where adsorption and desorption can be significant. We hope that the ideas presented here will inspire new experiments of these kinds of dispersion problems for colloidal suspensions.

* * *

This publication is based on work partially supported by Award No. KUK-C1-013-04, made by King Abdullah University of Science and Technology (KAUST). We gratefully acknowledge helpful discussions with J. M. Aristoff, W. Holloway, P. D. Howell, M. Reyssat, R. Rusconi and R. W. Style.

REFERENCES

[1] Russel, W. B., Saville, D. A. & Schowalter, W. R., *Colloidal Dispersions.*, edited by Cambridge Univ. Pr. 1992.
[2] Shipley, R. J.,Waters, S. L. & Ellis, M. J., *Biotech. Bioeng.*, **107** (2011) 382.
[3] Squires, T. M. and Quake, S. R., *Rev. Mod. Phys.*, **77** (2005) 977.
[4] Morris, J. F. & Brady, J. F., *Int. J. Multiphase Flow*, **24** (1998) 105.
[5] Gershenwald, J.E. *et al.*, *Surgery*, **124** (1998) 203.
[6] Kreuter, J., *Colloidal Drug Delivery Systems.* 1994.
[7] Karagas, M. R., *The Lancet*, **376** (2010) 213.
[8] Blatt, W. F., David, A., Michaels, A. S. & Nelson, L., *Membrane Science and Technology.* 1970.
[9] Henry, J. D., *Rec. Dev. Sep. Sci.*, **2** (1970) 205.
[10] Porter, M. C., *Ind. Eng. Chem. Prod. Res. Dev.*, **11** (1972) 234.
[11] Davis, R. H., & Sherwood, J. D., *Chem. Eng. Sci.*, **45** (1990) 3203.
[12] Räder, A. S., Tessaro, I. C , Damasceno, L. & Marczak, F., *Can. J. Chem. Eng.*, **89** (2011) 139.
[13] Taylor, G., *Proc. Roy. Soc. A*, **219** (1953) 186.
[14] Aris, R., *Proc. Roy. Soc. A*, **38** (1956) 67.
[15] Brenner, H. & Edwards, D. A., *Macrotransport Processes*, edited by Butterworth-Heinemann. 1993.
[16] Cook, B. P., *Phys. Rev. E.*, **78** (2008) 045303.
[17] Eckstein, E. C., Bailey, D. G. & Shapiro, A. H., *J. Fluid Mech.*, **79** (1977) 191.
[18] Leighton, D. & Acrivos, A., *J. Fluid Mech.*, **177** (1986) 109.
[19] Leighton, D. & Acrivos, A., *J. Fluid Mech.*, **181** (1986) 415.
[20] Lopez, M. & Graham, M. D., *Phys. Fluids*, **19** (2007) 073602.
[21] Rusconi, R. & Stone, H. A., *Phys. Rev. Lett.*, **101** (2008) 254502.
[22] Wedin, P. *et al.*, *J. Colloid Int. Sci.*, **272** (2004) 1.
[23] Barenblatt, G. I., *Prikl. Mat. Mekh*, **16** (1952) 67.
[24] Pattle, R. E., *Q. J. Mech. Appl. Math.*, **12** (1959) 407.
[25] Belongia, B. M. & Baygents, J. C., *J. Colloid Int. Sci.*, **195** (1997) 19.
[26] d'Orlyé, F., Varenne, A. & Gareil, P., *J. Chromatography A*, **1204** (2008) 226.
[27] Appell, J., Porte, G. & Buhler, E., *J. Phys. Chem. B.*, **109** (2005) 13186.
[28] Petsev, D. N. & Denkov, N. D., *J. Colloid Int. Sci.*, **149** (1992) 329.

RECENT REPORTS

57/11	Isolating intrinsic noise sources in a stochastic genetic switch	Newby
58/11	Riemann-Cartan Geometry of Nonlinear Dislocation Mechanics	Yavari Goriely
59/11	Helices through 3 or 4 points?	Goriely Neukirch Hausrath
60/11	Bayesian data assimilation in shape registration	Cotter Cotter Vialard
61/11	Asymptotic solution of a model for bilayer organic diodes and solar cells	Richardson Please Kirkpatrick
62/11	Neural field model of binocular rivalry waves	Bressloff Webber
63/11	Front propagation in stochastic neural fields	Bressloff Webber
64/11	Stability estimates for a twisted rod under terminal loads: a three-dimensional study	Majumdar Prior Goriely
65/11	Adaptive Finite Element Method Assisted by Stochastic Simulation of Chemical Systems	Cotter Vejchodsky Erban
66/11	On the shape of force–free field lines in the solar corona	Prior Berger
67/11	Tear film thickness variations and the role of the tear meniscus	Please Fulford Fulford Collins
68/11	Comment on “Frequency-dependent dispersion in porous media”	Davit Quintard
69/11	Molecular Tilt on Monolayer-Protected Nanoparticles	Giomi Bowick Ma Majumdar
70/11	The Capillary Interaction Between Two Vertical Cylinders	Cooray Cicuta Vella
71/11	Nonuniqueness in a minimal model for cell motility	Gallimore Whiteley Waters King Oliver
72/11	Symmetry of uniaxial global Landau-de Gennes minimizers in the theory of nematic liquid crystals	Henao Majumdar

01/12	Mechanical growth and morphogenesis of seashells	Moulton Goriely Chirat
02/12	How linear features alter predator movement and the functional response	McKenzie1 Merrill Spiteri Lewis
03/12	The Fourier transform of tubular densities	Prior Goriely
04/12	Numerical studies of homogenization under a fast cellular flow.	Iyer Zygalakis
05/12	Solute transport within porous biofilms: diffusion or dispersion?	Davit Byrne Osborne Pitt-Francis Gavaghan Quintard
06/12	Effects of intrinsic stochasticity on delayed reaction-diffusion patterning systems	Woolley Baker Gaffney Maini Seirin-Lee

Copies of these, and any other OCCAM reports can be obtained from:

Oxford Centre for Collaborative Applied Mathematics
Mathematical Institute
24 - 29 St Giles'
Oxford
OX1 3LB
England
www.maths.ox.ac.uk/occam